THERMAL BEHAVIOR OF BRANNERITE CERAMICS AND ITS NATURAL ANALOGUE MINERAL BRANNERITE

VLADIMÍR BALEK*, **, VLADIMÍR ZELEŇÁK**, ****, MARTIN BENEŠ**, JAN ŠUBRT***

**Nuclear Research Institute Řež , plc , 250 68 Řež , Czech Republic*
***Research Center Řež , Ltd., 250 68, Řež, Czech Republic*
****Institute of Inorganic Chemistry, ASCR, 250 68, Řež, Czech Republic*
***** Faculty of Sciences, P.J. Šafárik University, Moyzesova 11, 041 54 Košice, Slovak Republic*

E-mail: bal@ujv.cz

Submitted July 2007; accepted October 27, 2008

Keywords: Brannerite ceramics, Brannerite mineral, Emanation thermal analysis, Microstructure, Thermal behavior

Thermal behavior of brannerite ceramics (uranium titanate of chemical composition UTi_2O_6) was characterized in the range 30-1250°C. By using emanation thermal analysis (ETA) the temperatures of the microstructure changes were indicated as a decrease of radon release rate, the onset of healing subsurface microstructure irregularities is supposed at 250°C, whereas the onset of sintering at 800°C. The intensity of microstructure changes in the temperature intervals 250-500°C and 800-950°C was assessed by a mathematical model. From the ETA results of metamict brannerite mineral (from locality El Cabril near Cordoba, Spain) it followed that in the range 970-1020°C the crystallization of the metamict mineral took place. Relative changes in the amount of microstructure irregularities during heating of the metamict brannerite mineral were assessed from the ETA results measured on heating and subsequent cooling to temperatures of 300, 550, 750, 880, 1020 and 1150°C, respectively.

INTRODUCTION

Brannerite (uranium titanate, UTi_2O_6) is a minor phase in titanate-based ceramics designed for the geological immobilization of surplus plutonium or high level radioactive waste (HLW) resulting from nuclear industry facilities [1-4]. The structure of brannerite can be described considering TiO_6 and UO_6-octahedra (see Figure 1). Edge-sharing TiO_6-octahedra form sheets, which are connected by U cations located at the interlayer sites and coordinated by six oxygen atoms. UO_6-octahedra are nearly regular in shape and share edges much like the octahedra in rutile. Each Ti octahedron shares three edges with adjacent Ti octahedra and three corners with U octahedra. The U octahedra share two edges with neighboring UO_6 octahedra and four corners with TiO_6 octahedra. The brannerite mineral has the general formula $U_{1-x}Ti_{2+x}O_6$ and can be found in nature as metamict due to α-decay damage caused by the high content of uranium and thorium elements. Natural brannerite generally contains impurity elements like Pb, Ca, Th, Y on the U-site and Si, Al and Fe on the Ti-site [5].

In this paper emanation thermal analysis (ETA) has been used to characterize the thermal behavior, transport properties and annealing of microstructure irregularities of the brannerite ceramics and of a metamict brannerite mineral on heating in argon.

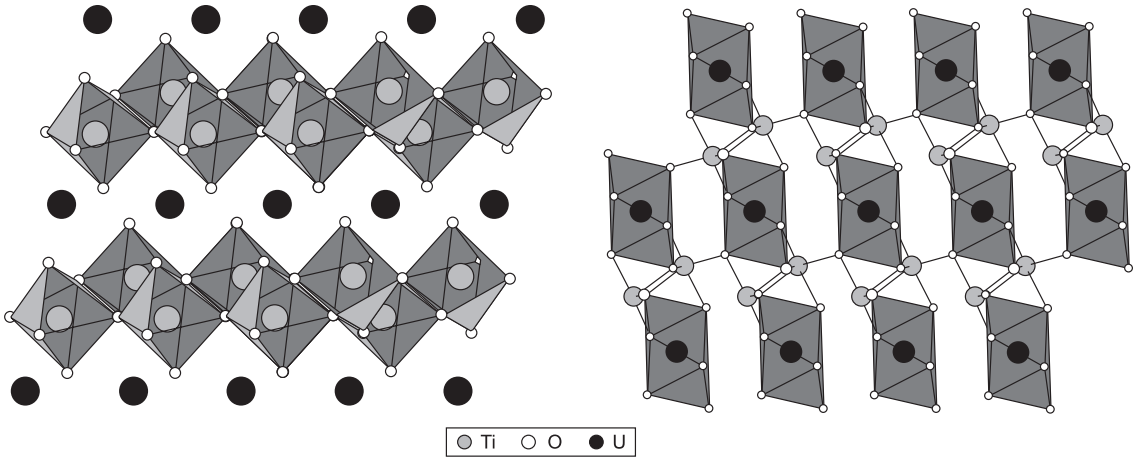

Figure 1. Scheme of (a) TiO_6 and (b) UO_6 octahedra in the structure of brannerite.

EXPERIMENTAL

Samples

Brannerite ceramics (chemical composition UTi_2O_6) was prepared from the stoichiometric mixture of UO_2 and TiO_2 (anatase). The mixture was calcined in argon at 750°C for 1 hour and subsequently wet-milled for 2 hours and dried. The sample contained mainly brannerite phase with minor rutile inclusions (~5% TiO_2) and trace amounts of uranium(IV) oxide (< 0.1%). The grain size of the powdered sample was 75-150 μm. The surface area of the sample, determined by the B.E.T. method, was 0.08 $m^2\ g^{-1}$. According to XRD results the sample was crystalline brannerite containing some amount of the amorphous phase.

Natural brannerite mineral was from the locality El Cabril mine, Spain. The sample was X-ray amorphous and contained Ca, Pb and other impurity elements. It was of general formula $U_{1-x}Ti_{2+x}O_6$ [6-8].

Methods

ETA measurements were carried out by using the updated NETZSCH DTA-ETA equipment Type 404. Details of ETA measurements have been described elsewhere [9, 10]. The ETA involves measurements of radon release rate from samples. The samples were labeled by traces of ^{228}Th as nitrate from the acetone solution. Atoms of radon, ^{220}Rn, were formed by a spontaneous α-decay of ^{228}Th and ^{224}Ra and were incorporated into the sample using the recoil energy of 85 keV $atom^{-1}$. The maximum depth of ^{220}Rn penetration was 80 nm as calculated with Monte Carlo method using TRIM code [11].

The specific activity of the sample was 10^5 Bq per gram. The sample (amount 0.1 g) was heated at the rate of 6 K min^{-1} in argon. Thermogravimetry measurement of the mineral brannerite sample was carried out by using NETZSCH STA 404 equipment. The sample amount 0.043 g was heated an alumina crucible at the rate of 6 K min^{-1}. SEM micrographs were obtained with PHILIPS equipment (Type XL 30CP).

Evaluation of the ETA results

The temperature dependence of the radon release rate, $E(T)$, can be expressed as

$$E(T) = E_{RT} + E_D(T)\Psi(T) \quad (1)$$

where E_{RT} is the radon release rate measured at room temperature, being proportional to the external surface area of the sample, $E_D(T)$ is the radon release rate due to diffusion along structure irregularities that served as radon diffusion paths, $\Psi(T)$ function is related to the changes in the amount of radon diffusion paths.

The temperature dependence of the radon release obtained by ETA was used for the evaluation of the transport properties and for microstructure development characterization of the samples on heating. Following equations were used for fitting with the experimental ETA data.

The radon release rate due to diffusion, $E_D(T)$, was expressed as

$$E_D(T) = A[F(T_0) - F(T)] \quad (2)$$

where $F(T) = 1/k_{D0} \exp(-Q_D/RT) + \lambda_{Rn}$, $A = \lambda_{Ra}C_{Ra}$ is the change in ^{224}Ra concentration, where $\lambda_{Ra} = 2.2035 \times \times 10^{-6}$ (s^{-1}) is the decay constant of ^{224}Ra, C_{Ra} is the equilibrium concentration of ^{224}Ra, and $\lambda_{Rn} = 1.2464 \times \times 10^{-2}$ (s^{-1}) is the decay constant of ^{220}Rn; T_0 is the initial temperature of heating, k_D is the rate constant of radon diffusion, depending on temperature according to the Arrhenius relationship,

$$k_D = k_{D0} \exp(-Q_D/RT) \quad (3)$$

where Q_D is the activation energy of radon diffusion, $R = 8.314$ $Jmol^{-1}\ K^{-1}$ is the universal gas constant.

For the description of changes in the amount of radon diffusion paths on the sample heating the following $\Psi(T)$ function was used

$$\Psi(T) = 1 - \frac{\kappa}{2}\left[1 + erf\frac{1 - \frac{T_m}{T}}{\frac{\Delta T\sqrt{2}}{T}}\right] \quad (4)$$

where erf denotes the Gauss error function, T_m is the temperature of maximum rate of the healing of the defects which serve as radon diffusion paths, ΔT is the temperature interval of the respective solid state process and κ is a theoretical parameter describing the contribution of the respective solid state process to the change in the number of the radon diffusion paths.

In general, the increase in the radon release rate, E, may characterize an increase of the surface area of interfaces, whereas a decrease in E may reflect processes like closing up structure irregularities that serve as paths for radon migration, closing pores and/or a decrease in the surface area of the interfaces.

RESULTS AND DISCUSSION

Thermal behavior of brannerite ceramics

Figure 2 depicts the ETA experimental data (points) of the brannerite ceramics sample measured on heating and subsequent cooling in argon and the ETA results obtained by fitting [12] with the mathematical model (full lines). The increase of the radon release rate $E(T)$ observed in the temperature range 20-250°C was due to the radon diffusion along subsurface structure irregularities that served as radon diffusion paths. It was assumed that the radon diffusion in this temperature range was controlled by a random "single jump" mechanism. The break observed at about 250°C and

the subsequent decrease of the radon release rate $E(T)$ in the range 250-500°C are due to thermal healing of subsurface microstructure irregularities that served as radon diffusion paths.

From SEM micrographs (Figure 3) it followed that the surface microstructures of the brannerite ceramics sample before heating and of the sample heated to 480°C were similar. We supposed that on sample heating above 500°C the increase of the radon release rate $E(T)$ was due to the radon diffusion along grain boundaries. The break observed at about 800°C and the subsequent decrease of $E(T)$ was ascribed to the sintering of the ground brannerite ceramics. The SEM micrograph of the sample heated to 1000°C (Figure 3) supported this interpretation. In its turn, the enhanced radon release observed in the range 1000-1250°C was due to radon diffusion in the bulk of the sample.

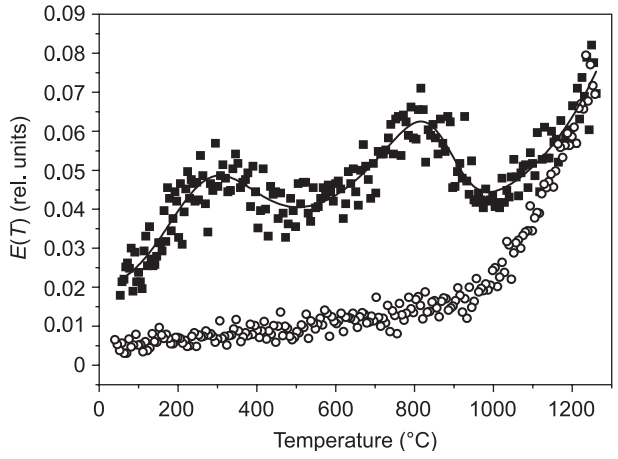

Figure 2. ETA results of brannerite ceramics sample fitted with the mathematical model; full points represent the ETA experimental data (squares - heating; circles - cooling), the full line corresponds to fitted results of the temperature dependence of the emanation rate.

From the ETA results measured on sample cooling from 1250 to 30°C (Figure 2) it is obvious that processes that took place on heating of the brannerite ceramics sample are irreversible.

In the interpretation of the ETA results fitted with the mathematical model [12,13] we supposed that the radon release from the solid is controlled by several mechanisms, namely by a "single jump" random diffusion in surface and subsurface of the sample (in the range 50-250°C), by diffusion via grain boundaries (in the range 500-800°C) and by a bulk diffusion mechanism (in the range 1000-1250°C), respectively. Table 1 summarizes the values of radon diffusion parameters determined from the ETA data that were measured on heating in the respective temperature intervals. Radon atoms served as a tracer of the brannerite ceramics permeability for species of the comparable size to radon atoms (i.e. 0.38nm), e.g. water molecules.

Figure 4 depicts temperature dependences of the $\Psi(T)$ functions characterizing the decrease of the amount of radon diffusion paths due to healing of subsurface microstructure irregularities (curve a - maximum rate at 320°C) and due to sintering on heating above 700°C (curve b - maximum rate at 861°C).

Thermal behavior of brannerite mineral

Figure 5 shows ETA results of the sample of mineral brannerite measured during heating in argon in the range 20-1200°C and subsequent cooling. The increase of radon release rate, E, observed on sample heating in the range of 40-300°C characterized the diffusion mobility of radon atoms along surface cracks and other subsurface defects to the depth of 80 nm.

The slight decrease of $E(T)$ observed in the curve 1a Figure 5 in the temperature range of 400-500°C was ascribed to healing surface cracks and voids. The decrease of the radon release rate $E(T)$ observed on the

Table 1. Parameters of radon mobility in brannerite ceramics samples evaluated from ETA measurements.

Heating in the temperature range					
20-250°C		500-800°C		1000-1250°C	
k_0 (cm^2/s)	Q_D (kJ/mol)	k_0 (cm^2/s)	Q_D (kJ/mol)	k_0 (cm^2/s)	Q_D (kJ/mol)
2.2 × 10-9	40 ± 3	6.2 × 10-6	143 ± 2	1.3 × 10-5	230 ± 3

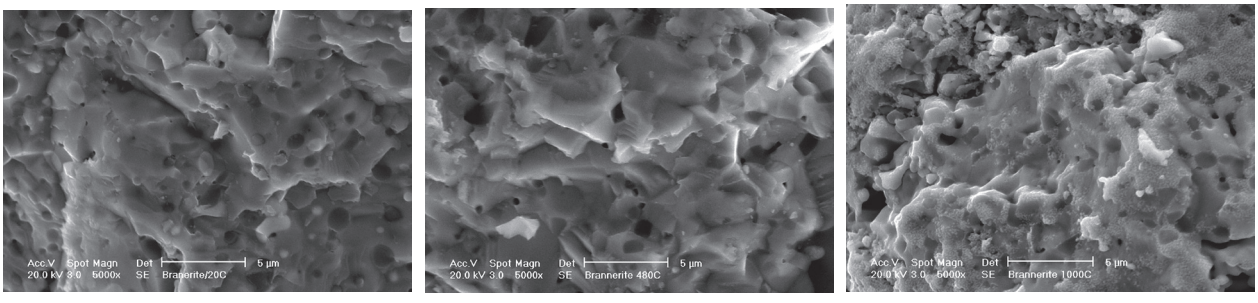

20°C 480°C 1000°C

Figure 3. SEM micrographs of brannerite ceramics sample heated to various temperatures.

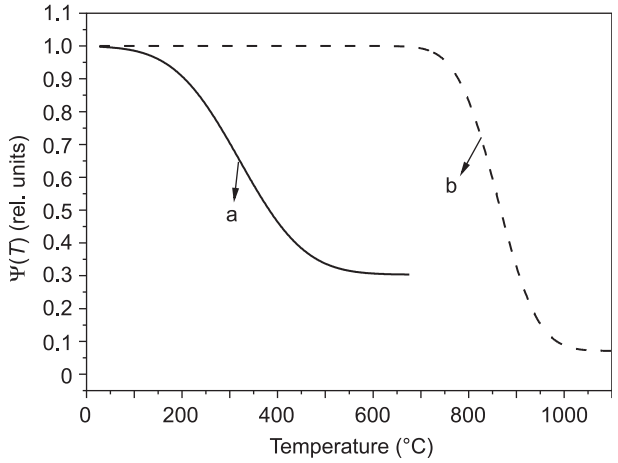

Figure 4. Ψ(*T*) functions obtained by fitting the ETA experimental data corresponding to the healing of subsurface microstructure irregularities (a) and to sintering of the sample (b).

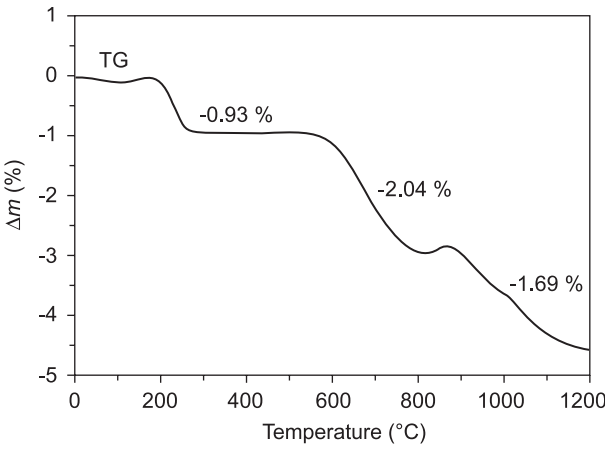

Figure 6. Results of TG obtained during heating of metamict brannerite mineral sample in argon.

ETA curve in the range 800-880°C, corresponding to the healing microstructure irregularities, was considered as a first step of the formation of crystalline brannerite. The increase of *E*(*T*) observed in range 900-965°C followed by the sharp decrease of *E*(*T*) in the range 970-1020°C indicated the formation of a crystalline brannerite phase [14]. From the comparison of the ETA results of the brannerite mineral sample measured on heating up to 1200°C (curve 1a, Figure 5) and subsequent cooling at the same rate (curve 1b, Figure 5) it followed that the microstructure changes on sample heating were irreversible.

From TG results (Figure 6) it followed that in the temperature ranges 200-300°C, 570-760°C and 840-1040°C, the respective mass loss values were: 0.93 %, 2.04 % and 1.69 %. The release of CO_2 was detected by mass spectrometry [14]. Consequently, a thermal degradation of minor carbonate containing components of the sample can be supposed. Moreover, we assumed that the mass decrease in the range 840-1040°C was associated with the decrease of the amount of Pb and Ca impurities. As it has been published in [8] the amount of CaO, PbO and other impurities of the brannerite mineral decreased on sample heating from 900°C to 1100°C. It should be mentioned that the release of CO_2 observed in the temperature range before the sample re-crystallization gave rise to the sample porosity [14]. The microstructure changes associated with the changes of the sample porosity characterized by ETA during heating and subsequent cooling in the selected temperature intervals are presented in Figure 5.

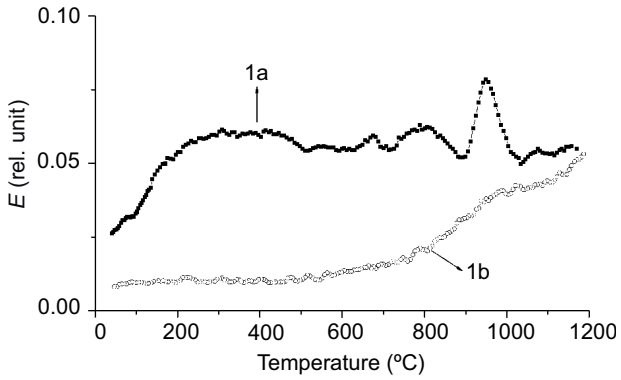

Figure 5. ETA results of metamict brannerite mineral sample measured on heating (curve 1a) and subsequent cooling (curve 1b) in argon in the range 20-1200°C.

Differences in the microstructure of the brannerite mineral sample before and after heating to 1200°C were observed in the SEM micrographs (Figure 7).

It was of interest to investigate the metamict brannerite mineral during "step by step" heating and subsequent cooling of the sample to the temperatures of 300, 550, 750, 880, 1020 and 1150°C, respectively (Figure 8). As follows from the ETA results in Figure 8 the "step by step" heating of the sample to these temperatures caused a decrease of the amount of structure irregularities serving as radon diffusion paths.

A good reproducibility of the ETA results measured on heating from 20 to 300°C is obvious from the comparison of the results in Figure 8, curve 2a and curve 1a.

The ETA curves 3a/3b, 4a/4b and 5a/5b in Figure 8 characterized the thermal behavior of brannerite sample pre-heated to 300, 550 and 750°C, respectively. The increase of the emanation rate, *E*, in the temperature range of 20-360°C, corresponding to the diffusion of radon along micropores in the sample, was followed by the decrease of *E*, characterizing the partial healing of voids and structure irregularities that served as diffusion pathways for radon.

The ETA curves 6a/6b in Figure 8 characterized the thermal behavior of the sample pre-heated to 880°C. As already observed by curve 1a in Figure 8 the structure irregularities serving as radon diffusion paths were further diminished in the sample pre-heated to 880°C. The increase of the emanation rate on sample heating

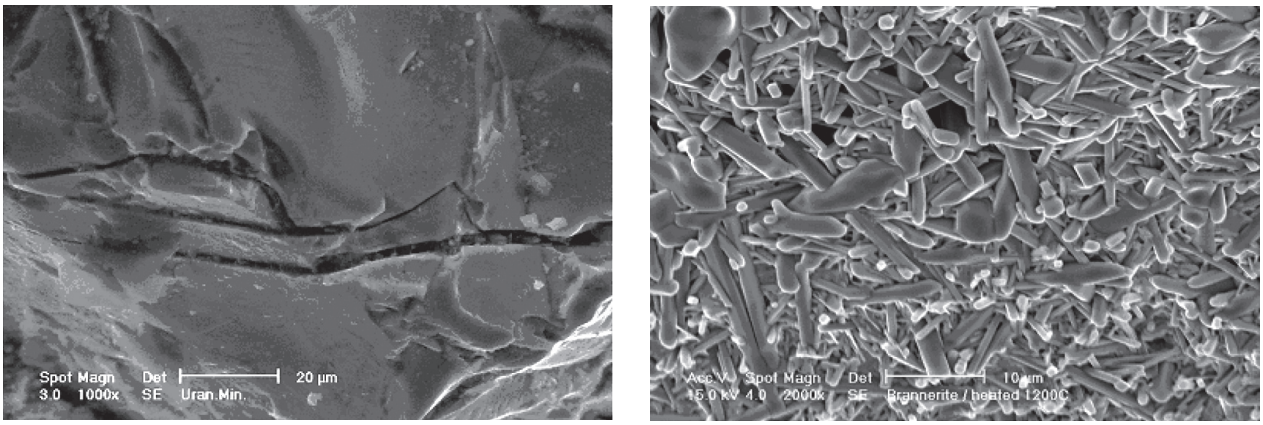

a) b)

Figure 7. SEM micrographs of brannerite mineral sample; a) as received, b) heated to 1200°C.

above 600°C reflected an enhanced radon diffusion in the sample matrix, whereas the sharp decrease observed on heating above 970-1020°C indicated the next step of the formation of crystalline brannerite. A good reproducibility of the ETA measurements can be seen from the temperature coincidence of the effects on the curve 1a and the curve 6a in Figure 8.

From curves 7a/7b in Figure 8, characterizing the thermal behavior of the sample pre-heated to 1020°C, it is obvious that after the pre-heating the sample to this temperature an irreversible crystallization of amorphous brannerite mineral took place.

As is obvious from Table 2, the amount of structure irregularities serving as radon diffusion paths further diminished, and the radon permeability in the brannerite mineral sample decreased. It should be mentioned here that the emanation thermal analysis revealed sensitively the differences in the amount of structure irregularities that served as radon diffusion paths in the amorphous brannerite mineral sample.

Values of the emanation rate E_{RT} measured at room temperature before and after each heating run were used for the assessment of the relative changes of the surface area affected by the respective heat treatments. The E_{RT} values summarized in Table 2 are in agreement with our considerations of the annealing of surface area and subsurface irregularities.

It should be pointed out that the emanation thermal analysis sensitively revealed the differences in the amount of structure irregularities that served as radon diffusion

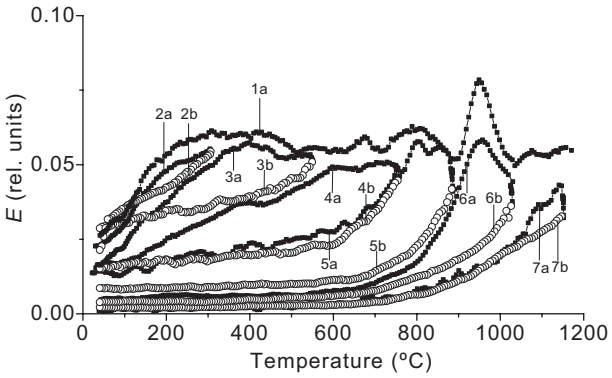

Figure 8. Emanation thermal analysis results of metamict brannerite mineral sample measured on heating and subsequent cooling in argon in the range 20-1150°C: curve 1a was measured of "as received" sample during heating from 20 to 1150°C, curves 2a/2b, 3a/3b, 4a/4b, 5a/5b, 6a/6b and 7a/7b were measured with a parallel samples pre-heated to the temperatures of 300, 550, 750, 880 and 1020°C, respectively.

Table 2. Defect amount characteristics of brannerite mineral sample pre-heated to various temperatures.

ETA curves measured on heating/cooling	Temperature of sample pre-heating	Defect amount characteristics ξ*	E_{RT} (rel. units)	Δξ** (%)
Curves 1a/1b, Figure 5	as received	38.1	0.026	100
Curves 2a/2b, Figure 8	as received	0.41	0.023	1.08
Curves 3a/3b, Figure 8	300°C	3.82	0.017	10.02
Curves 4a/4b, Figure 8	550°C	10.26	0.015	26.93
Curves 5a/5b, Figure 8	750°C	13.62	0.014	35.75
Curves 6a/6b, Figure 8	880°C	6.30	0.005	16.54
Curves 7a/7b, Figure 8	1020°C	0.98	0.001	2.57

* $\xi(T_{max}) = \int_{T_{min}}^{T_{max}} E(T)_{heating}\,dT - \int_{T_{min}}^{T_{max}} E(T)_{cooling}\,dT$ ** $\Delta\xi = \frac{\xi_n}{\xi_1} \times 100$ (%)

paths in the sample. From the temperature dependences of the radon release rate $E(T)$, measured during heating to the selected temperatures and subsequent cooling, the decrease in the amount of radon diffusion paths was assessed. To this aim we used the parameter ξ defined in Equation (5) as:

$$\xi(T_{\max}) = \int_{T_{\min}}^{T_{\max}} E(T)_{heating}\, dT - \int_{T_{\min}}^{T_{\max}} E(T)_{cooling}\, dT \qquad (5)$$

Moreover, values of $\Delta\xi$ (see Equation (6)) were calculated with the aim to compare the amounts of the annealed microstructure defects during the "step by step" heating of the sample. The difference of integrals used for the assessment of the amount of the microstructure defects can be expressed as $\Delta\xi$ defined as

$$\Delta\xi = \frac{\xi_n}{\xi_1} \times 100 \ \ (\%) \qquad (6)$$

As it followed from values of ξ and $\Delta\xi$ summarized in Table 2, the most significant decrease of the structure irregularities serving as diffusion paths for radon diffusion was annealed prior to the crystallization of the sample in the range of 970-1020°C.

It was shown that the emanation thermal analysis revealed the differences in the amount of structure irregularities that served as radon diffusion paths in the metamict brannerite mineral.

CONCLUSIONS

By using emanation thermal analysis (ETA) the healing microstructure irregularities of the brannerite based ceramics was indicated by a decrease of radon release rate: the onset of healing subsurface microstructure irregularities at 250°C and the onset of the sample sintering at 800°C. The transformation of metamict mineral brannerite to crystalline brannerite was indicated by a break on the ETA curve in the temperature range 970-1020°C, in agreement with the XRD results. Moreover, relative changes in the amount of microstructure irregularities in the amorphous of the brannerite mineral sample were assessed from the ETA results measured during heating and subsequent cooling to selected temperatures in the range from 300 to 1130°C. The emanation thermal analysis sensitively revealed the differences in the amount of structure irregularities that served as radon diffusion paths in the metamict brannerite mineral.

Acknowledgement

This work was supported by the Ministry of Education, Youth and Sports of the Czech Republic (Project MSM-2672244501, LA-292 and ME - 879) and the Academy of Sciences of the Czech Republic (Project AV0Z403005). Authors thank Prof. I.N. Beckman and Dr. I.M.Bountseva, Moscow State University for valuable discussions.

References

1. Ringwood A. E., Kesson S. E., Reeve K. D., Levins D. M., Ramm E. J. in: *Radioactive Waste Forms for the Future*, p. 233, Ed. Lutze W., Ewing R.C., Elseviser Science B.V. Amsterdam 1988.
2. Helean K. B., Navrotsky A., Lumpkin G. R., Colella M., Lian J., Ewing R. C., Ebbinghaus B., Catalano J. G.: J. Nucl. Mater. *320*, 1 (2003).
3. Szymanski J. T., Scott J. D.: Canad. Mineral. *20*, 271 (1982).
4. Lumpkin G. R., Leung S. H. F., Colella M.: Mat. Res. Soc. Symp. Proc. *608*, 359 (2000).
5. Ifill R. O., Cooper W. C., Clark A. H.: Chim Bull. *89*, 93 (1996).
6. Vance E. R., Stewart M. W. A., Day R. A., Hart K. P., Hambley M. J., Brownscombe A.: "Pyrochlore-rich Titanate ceramics for Incorporation of Plutonium, Uranium and Process Chemicals", Report of Australian Nuclear Science and Technology Organization, Sydney 1997.
7. Vance E. R., Watson J. N. Carter M. L., Day R. A. Lumpkin G. R., Hart K. P., Zhang Y., McGlinn P. J., Stewart M. W. A., Cassidy D. J. in: *Environmental Issues and Waste Management Technologies V*, pp. 561-568, Ed. Spearing D., American Ceramic Society, Westerville 2000.
8. Zhang Y., Lumpkin G. R., Li H., Blackford M. G., Colella M., Carter M. L., Vance E. R.: J. Nucl. Mat. *350*, 293 (2006).
9. Balek V., Brown M. E.: Less common techniques, in: *Handbook on Thermal analysis and Calorimetry*, Vol.1 Chapter 9, p.445, Ed. Brown M.E., Elseviser Science B.V. Amsterdam 1998.
10. Balek V., Mitamura H., Banba T., Beneš M., Málek Z., Beckman I.N., Bountseva I.M., Mitsuhashi T.: J. Therm. Anal. Cal. 80, 649 (2005).
11. Ziegler J.F., Biersack J.P and Littmark U.: *The Stopping and Range of Ions in Solids*, Pergamon Press, New York 1985.
12. Beckman I. N., Balek V.: J. Therm. Anal. Cal. *67*, 49 (2002).
13. Balek V., Klosová E., Beneš M., Šubrt J.: Ceramics-Silikáty *52*, 85 (2008).
14. Balek V., Vance E. R., Zeleňák V., Málek Z., Šubrt J.: J. Therm. Anal. Cal. *88*, 93 (2007).